Biochimica et Biophysica Acta, 955 (1988) 119–127
Elsevier

BBA 33155

Fluorescence studies on the dissociation and denaturation of pigeon liver malic enzyme

Hwei-Jen Lee [a], Yee-Hsiung Chen [b] and Gu-Gang Chang [a]

[a] *Department of Biochemistry, National Defense Medical Center and* [b] *Institute of Biological Chemistry, Academia Sinica and Institute of Biochemical Sciences, National Taiwan University, Taipei (Taiwan, China)*

(Received 11 January 1988)

Key words: Malic enzyme; Fluorescence; Subunit dissociation; Protein denaturation; Protein conformation; (Pigeon liver)

Exposure of pigeon liver malic enzyme ((*S*)-malate: $NADP^+$ oxidoreductase (oxaloacetate-decarboxylating), EC 1.1.1.40) in medium concentrations of guanidine-HCl at 25 °C and pH 7.45 caused biphasic conformational changes of the enzyme molecule. Molecular weight determination confirmed that the enzyme tetramers were dissociated to monomers in phase I transition. Enzymatic activity was completely lost in this phase. Recovery of the enzyme activity was only possible in the early stages of the phase I transition. Phase II was due to enzyme unfolding, as judged by circular dichroism and the fluorescence parameters of the enzyme. The steps of the transformation of native malic enzyme into a completely denatured state were in the following sequence: tetramer → monomer → random coil. Extensive denaturation of the enzyme molecule resulted in irreversible aggregation. Dissociation and denaturation were accompanied by a red-shift of the fluorescence spectrum (328 → 368 nm). Fluorescence quenching studies indicated that tryptophan residues of the enzyme molecule were buried deeply in the interior of the molecule. The tryptophan residues were only partially accessible by acrylamide and almost inaccessible by KI. Dissociation and denaturation were accompanied by exposure of the tryptophan residues, as manifested by the accessibility of the enzyme molecule toward KI or acrylamide.

Introduction

Pigeon liver malic enzyme ((*S*)-malate: $NADP^+$ oxidoreductase (oxaloacetate-decarboxylating), EC 1.1.1.40) has been found to be a tetrameric protein with identical subunits [1,2] (for review, see Ref. 3). The enzyme was dissociated into its constituent monomers in an acidic environment. Reassociation could be accomplished simply by adjusting the pH to neutrality [4]. We have used fluorescence quenching techniques to monitor the protein conformational changes [5]. A biphasic phenomenon was observed when the enzyme was treated with guanidine-HCl. In this paper, the biphasic denaturation of this enzyme is further characterized. The two phases were due to dissociation of the subunits and unfolding of the protein molecule, respectively.

Materials and Methods

Materials. Guanidine-HCl, KI and dimethylsulfoxide were purchased from E. Merck (Darmstadt, F.R.G.). Acrylamide (4 × recrystallized) was obtained from Fluka (Buchs, Switzerland). 3,3′-

Correspondence: Gu-gang Chang, Department of Biochemistry, National Defense Medical Center, P.O. Box 8244, Taipei, Taiwan, China.

Dithiobis(propionic acid *N*-hydroxysuccimide ester), 5,5′-dithiobis(2-nitrobenzoic acid), sodium thiosulfate and sodium dodecyl sulfate (SDS) were purchased from Sigma (St. Louis, MO, U.S.A.). Protein standards for molecular weight determination were purchased from Pharmacia (Uppsala, Sweden). All other chemicals were of reagent grade. Distilled deionized water was used throughout this work.

Malic enzyme from pigeon liver was purified according to our published procedure [6]. The purified enzyme was routinely checked for purity by polyacrylamide gel electrophoresis. Protein concentration was determined spectrophotometrically at 278 nm, using a molar absorption coefficient (tetramer) of $2.236 \cdot 10^5$ for the protein solution [7].

Enzyme assay. Malic enzyme activity was assayed at 30 °C according to Hsu and Lardy [7]. The formation of NADPH was monitored continuously at 340 nm in a Gilford 2600 spectrophotometer.

Denaturation of the enzyme. Denaturation of the enzyme by guanidine-HCl was performed by incubating the enzyme in 30 mM Tris-HCl buffer (pH 7.45) with guanidine-HCl (pH 7.5) at room temperature. When guanidine-HCl concentration was at least 2 M, all enzymatic activity was lost in 1 min. The denaturation time was usually 30 min, but in some experiments, overnight incubation was performed to ensure complete denaturation.

Dissociation of the enzyme. Dissociation of the enzyme by changing pH was performed by rapid dilution (20-fold) of the enzyme solution with potassium acetate buffer (pH 4.5). The dissociation process was instantaneous [4]. pH measurements were performed with a Radiometer PHM 84 research pH meter.

Cross-linking of the enzyme subunits and molecular-weight determination. In the pH dissociation experiments, chemical cross-linking of any associated subunits was performed with glutaraldehyde according to Hermann et al. [8]. After cross-linking, the enzyme solution was subjected to polyacrylamide disc-gel electrophoresis in the presence of SDS according to Weber and Osborn [9]. The stained gels were scanned at 560 nm with a Gilford 2600 spectrophotometer equipped with a 2410-S linear transport gel scanner.

Our previous studies demonstrated that pH changes caused a reversible and spontaneous dissociation–reassociation of the enzyme [4]. We therefore wish to analyse, by cross-linking experiments, the effect of guanidine-HCl on malic enzyme. To avoid the reaction of glutaraldehyde with high concentration of guanidine-HCl, another cross-linking agent, 3,3′-dithiobis(propionic acid *N*-hydroxysuccinimide ester) was used. The molar ratio of the reagent (dissolved in dimethyl sulfoxide) and the enzyme was 339. Cross-linking was performed in 0.2 M borate buffer (pH 8.0) for 10 min. The reaction was stopped by adding 80 mM glycine containing 2 mM 5,5′-dithiobis(2-nitrobenzoic acid). The enzyme solution was then dialysed exhaustively against 20 mM Tris-HCl buffer (pH 7.7) containing 1% glycerol. Dialysis to remove the guanidine-HCl was necessary, since a high concentration of guanidine-HCl would cause the precipitation of SDS. The dialysed sample was then subjected to disc-gel electrophoresis to determine the distribution of tetramers, dimers and monomers.

Fluorescence quenching studies. Quenching of protein intrinsic fluorescence by acrylamide or KI was performed at 30 °C using a Farrand system 3 thermoregulated spectrofluorometer. An excitation wavelength of 295 nm and emission wavelength of 340 nm were used. The enzyme was denatured to various degrees by incubating the enzyme with different concentrations of guanidine-HCl at 30 °C for 30 min or longer. The initial fluorescence (F_0) of the solution was measured. The enzyme fluorescence from the tryptophan residues (Trp) was then quenched by progressive addition of small aliquots (25 μl) of a concentrated solution of acrylamide or KI to the fluorimetric cuvette and the fluorescence intensity (F) measured again. At the concentrations used in fluorescence titration, the absorbance of KI at the excitation wavelength was not detectable, and thus no correction was necessary for the inner filter effect. The absorption of acrylamide at 295 nm was corrected according to Eqn. 1 [10]:

$$F_{corr} = F_{obs} 10^{\Delta A/2} \quad (1)$$

where $\Delta A/2$ was the increase in absorbance at the center of the cuvette caused by the addition of

acrylamide. The acrylamide used in these experiments had a molar absorption coefficient of 0.33 $M^{-1} \cdot cm^{-1}$ at 295 nm. Since the actual absorption was much lower than 0.2 A, the above simple correction equation should be valid [11].

Sodium thiosulfate (0.1 M) was added into the KI solution to prevent I_3^- formation. Ionic strength change caused by KI was corrected by the data obtained from separated experiments where quenching of the protein fluorescence by the same amount of NaCl was measured. When the quenching data were plotted according to the classical Stern-Volmer equation (Eqn. 2), downward Stern-Volmer plots were obtained.

$$F_0/F = 1 + K_{sv}[Q] \tag{2}$$

where [Q] was the quencher concentration and K_{sv} was the dynamic quenching constant. For monitoring protein conformational changes, the effective dynamic quenching constant ($K_{sv,eff}$) was used. $[(F_0/F) - 1]/[Q]$ was calculated for each [Q] according to Eqn. 3 and was plotted against [Q]. The data points were extrapolated to $[Q] = 0$. This initial slope of the Stern-Volmer plot represented a $K_{sv,eff}$, which was the average of the collisional quenching constants.

$$[(F_0/F) - 1]/[Q] = K_{sv} \tag{3}$$

Fluorescence quenching data were also fitted to Eqn. 4 for calculating various quenching parameters [10]:

$$F_0/\Delta F = 1/(f_a K_{sv}[Q]) + 1/f_a \tag{4}$$

where $\Delta F = F_0 - F$, and f_a was the fractional maximum accessible protein fluorescence [10,12].

Double quenching studies. Simultaneous quenching of protein fluorescence by KI and acrylamide was performed as described by Somogyi et al. [13]. KI was selected as the ionic quencher to selectively quench the emission of exposed tryptophan residues. Acrylamide was chosen as the nonionic quencher to quench both the exposed and masked fluorophors.

Acrylamide was added into enzyme solution immediately prior to titration with KI. The enzyme fluorescence was quenched by repetitive addition of small aliquots of 2.85 M KI stock solution, which contained same concentration of acrylamide as did the enzyme solution. Data from double quenching studies were fitted to Eqn. 5 [13]:

$$F_0/\Delta F = \frac{1 + K_{1e}[Q_1]}{\alpha} + \frac{(1 + K_{1e}[Q_1])^2}{\alpha K_2} \cdot \frac{1}{[Q_2]} \tag{5}$$

where $[Q_1]$ is the acrylamide concentration and $[Q_2]$ the KI concentration. K_{1e} represents the quenching constant for the external fluorophors. K_2 denotes the quenching constant for KI, and α represents the fraction of tryptophan residues accessible to KI. K_2 and α were estimated from experiments with KI as the only quencher, K_{1e} was calculated from double quenching experiments. Fitting of the experimental data to the above equations was carried out by least-squares method using the computer programs written by R.S. Chang [14]. Estimation of β (the fraction of tryptophan residues accessible only to acrylamide), K_{1i} (quenching constant for the internal fluorophors) and γ (the fraction of tryptophan residues inaccessible to both KI and acrylamide) were followed as described by Somogyi et al. [13] with acrylamide as the only quencher.

Circular dichroism studies. CD spectra were measured at 25°C with a Jasco J-20 spectropolarimeter under constant N_2 flush. Fused silica cylindrical cells of 0.5, 0.1 and 0.02 dm light paths were used to keep the absorbance of the solution below 2. Malic enzyme solution (1 mg/ml) was scanned from 300 to 190 nm. The scale of the recorder was changed according to the absorbance. When the analysis was completed, the buffer was scanned immediately to obtain the baseline. Denatured enzyme solution was filtered through a 0.45 mm filter (Whatman, U.K.) before analysis. Denaturing agent was included in the buffer to monitor the baseline for the denatured enzyme. Mean residue ellipticity was calculated according to Eqn. 6:

$$[\theta] = (M \cdot \theta)/(100 \cdot C \cdot l) \tag{6}$$

where l represents the light-path length (dm); M is the average molecular weight of the amino acids, a value of 111.15 being used for malic enzyme (calculated from Ref. 1); C is the con-

centration of malic enzyme (mg/ml); and θ is the optical rotation (deg · cm^2 · dmol^{-1}).

Calculation of the α-helix, β-pleated sheet and random coil content of the native enzyme was according to Greenfield and Fasman [15].

Results

Guanidine-HCl induced biphasic conformational change of malic enzyme

Guanidine-HCl at 2 M caused over 95% loss of the enzyme activity in 1 min. The CD spectrum of the native and guanidine-denatured enzyme was shown in Fig. 1. Curve A (right side) showed that the native enzyme had a absorption band between 300–250 nm characteristic for aromatic amino acids. The enzyme also showed the absorption of peptide chromophore located between 250–205 nm (left side) with two characteristic absorption peaks at 222 and 208 nm, indicating a highly ordered α-helical structure of the pigeon liver malic enzyme. To a first approximation, the α-helix of the enzyme was estimated to be 33%, which was consistent with the predicted value (37%) of rat liver malic enzyme obtained from the sequence data [16]. No β-pleated sheet was predicted for the rat liver enzyme [16]. The β-pleated sheet of pigeon liver malic enzyme was estimated to be below 15%. Curve B in Fig 1 showed that the regular structure of malic enzyme had completely collapsed in 3.5 M guanidine-HCl. Ellipticity at 222 nm ($[\theta]_{222}$) was used to represent the structural regularity of the enzyme molecule.

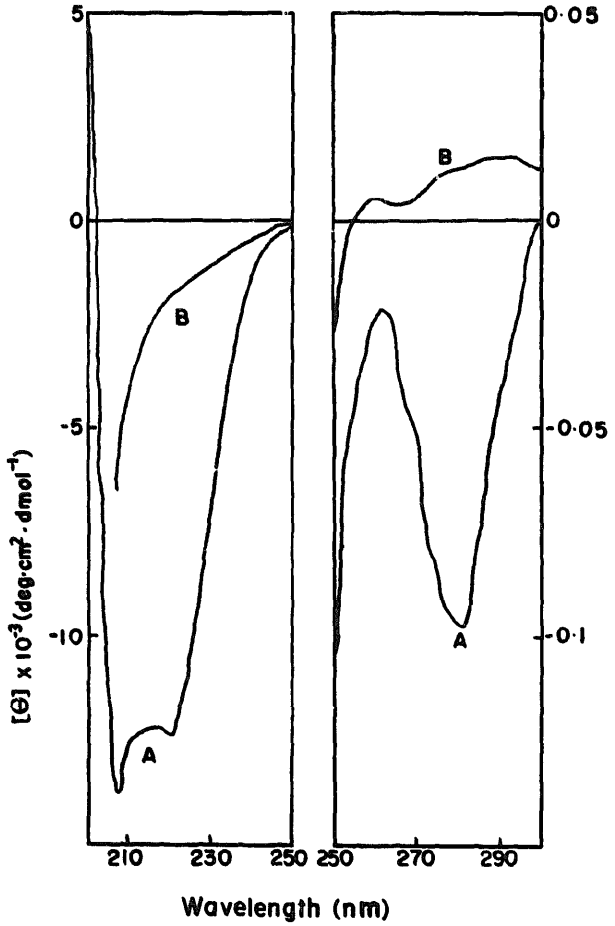

Fig. 1. Circular dichroism spectrum of malic enzyme. (A) Native enzyme (1 mg/ml) vs. buffer. (B) The enzyme denatured with 3.5 M guanidine-HCl vs. buffer containing the denaturing agent.

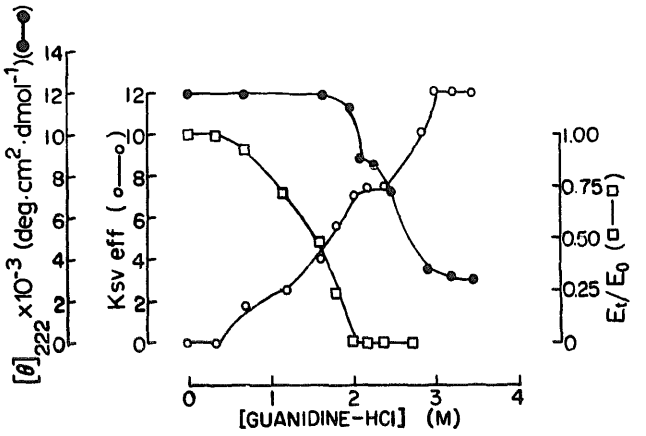

Fig. 2. Biphasic denaturation of malic enzyme. Malic enzyme was denatured to various stages with different concentrations of guanidine-HCl. The conformational changes of the enzyme molecule were monitored by effective dynamic quenching constant ($K_{sv,eff}$) for acrylamide, ellipticity ($[\theta]_{222}$), and enzymatic activity. E_0 and E_t represent enzyme activity at time zero and t, respectively.

Fig. 2 showed the changes of the enzyme structure in accordance with the concentrations of guanidine-HCl. The native enzyme had a highest structural regularity reflected by its highest absolute $[\theta]_{222}$ and lowest $K_{sv,eff}$ values. With the increase in guanidine concentration, $[\theta]_{222}$ decreased whereas $K_{sv,eff}$ increased. There was a inflection point around 2.0 ± 0.3 M guanidine-HCl. This experiment was repeated many times. There was always a bump at [guanidine-HCl] $\approx$ 2.0 M. Same results were obtained if the CD or fluorescence measurements were taken after 12 h. The biphasic process as shown by CD data, within experimental error, coincided exactly with the

fluorescence quenching results. The data shown in Fig. 2 indicated the reliability of using quenching of intrinsic protein fluorescence as a tool to monitor the protein conformational changes [5]. Attempts to show the reversibility of the transition were not successful. Enzymatic activity was completely lost in the first phase of the denaturation. Recovery of enzyme activity was only possible at early stage by diluting the denatured enzyme with 0.67 M triethanolamine-HCl buffer (pH 7.4) containing 0.5 M dithioerythritol and 50 mg/ml gelatin. Denaturation to phase II was essentially irreversible.

Molecular weight changes during denaturation and dissociation

Since malic enzyme is a tetrameric protein with identical subunits [2], the above experimental results prompted us to differentiate between dissociation of subunits and/or unfolding of the individual monomer to give the biphasic phenomenon. We determined the molecular weights of the enzyme denatured to various stages by SDS-electrophoresis, and used 3,3′-dithiobis(propionic acid *N*-hydroxysuccinimide ester) to cross-link the associated subunits. As shown in Fig. 3, [guanidine-HCl] $\geqslant$ 2 M induced dissociation of the enzyme. In other experiments the enzyme was shown to dissociate at 1.5 M (data not shown). The protein bands shown in Fig. 3 were diffused. This was because dialysis procedure increases the sample volume. In order to obtain enough sensitivity, a larger sample volume was applied during electrophoresis.

Acidic environments caused reversible dissociation of the enzyme, as demonstrated earlier [4]. Selected gel scan was shown in Fig. 4. In these experiments, the cross-linking agent used was glutaraldehyde which linked lysyl ε-amino groups.

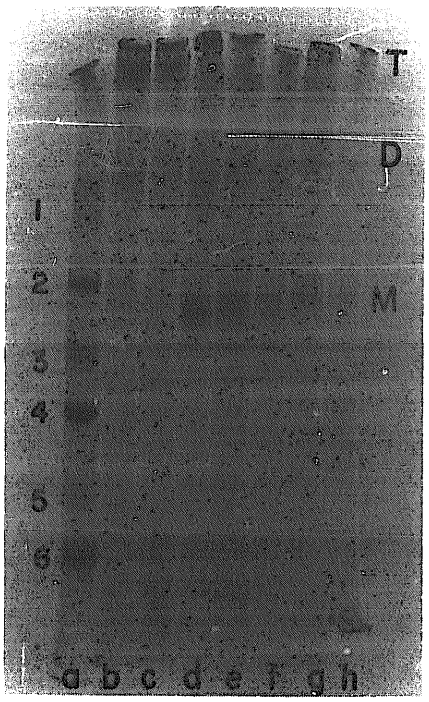

Fig. 3. Sodium dodecyl sulfate disc-gel electrophoresis of pigeon liver malic enzyme denatured by guanidine-HCl. The enzyme was subjected to SDS-electrophoresis after cross-linking. Gel concentration was 7.8%. Gel a, molecular weight standards. 1, phosphorylase *b* (M_r 94000); 2, bovine serum albumin (M_r 67000); 3, ovalbumin (M_r 43000); 4, carbonic anhydrase (M_r 30000); 5, trypsin inhibitor (M_r 20100); and 6, α-lactalbumin (M_r 14400). T, tetramers; D, dimers; and M, monomers. For gels b–h, the enzyme was denatured with 0, 1, 2, 3, 4, 5 and 6 M guanidine-HCl, respectively.

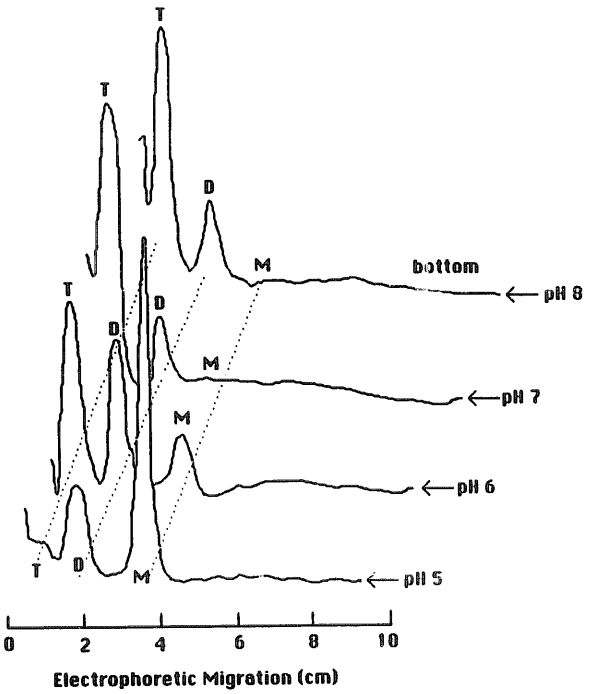

Fig. 4. Distribution of tetramers, dimers and monomers of pigeon liver malic enzyme at different pH. Malic enzyme was exposed to different pH buffers and the associated subunits cross-linked with glutaraldehyde. SDS-electrophoresis was used to separate the tetramers (T), dimers (D), or monomers (M). The stained gels were scanned at 560 nm with a densitometer. For clarity only selected gels were demonstrated.

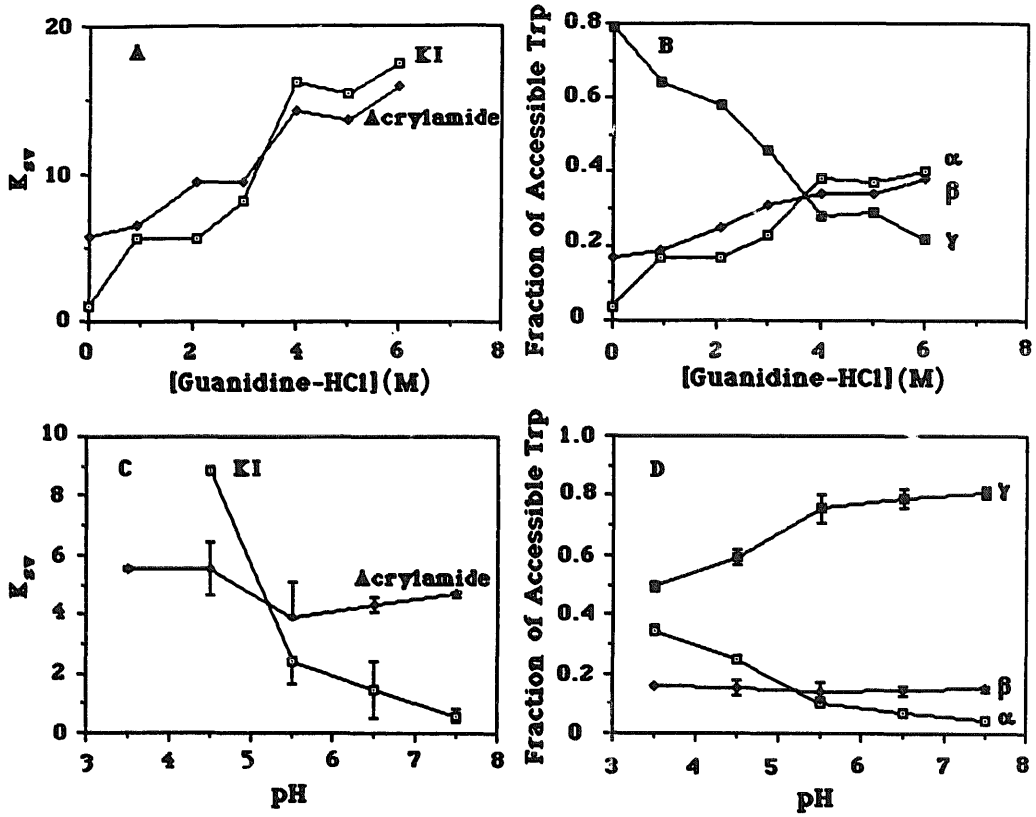

Fig. 5. Variation of dynamic quenching constants and fractional tryptophan residues accessibility of pigeon liver malic enzyme with guanidine-HCl concentration and pH. The enzyme was dissociated at acidic pH or denatured to various degrees with guanidine-HCl. The tryptophan fluorescence was quenched with KI or acrylamide. Dynamic quenching constant (A and C) or accessibility of tryptophan to KI (α), acrylamide (β) and inaccessible tryptophan (γ) (B and D) were plotted vs. [guanidine-HCl] (A and B) or pH (C and D).

Spectral change of malic enzyme after denaturation

The fluorescence emission spectra of the native, intermediate and unfolded conformation of pigeon liver malic enzyme were recorded. The native enzyme fluorescenced at 328 nm with a shoulder at 340 nm. Unfolding of the enzyme was accompanied by a red-shift of the fluorescence emission to 368 nm. The ratio of F_{368}/F_{328} increased with the increase in guanidine-HCl concentration. KI and acrylamide quenched both F_{368} and F_{328}.

The fluorescence spectrum of the enzyme at acidic pH was not available due to the interference of acetate buffer on the fluorescence.

Accessibility of tryptophan residues toward KI and acrylamide

Malic enzyme denatured to various degrees by guanidine-HCl treatment was quenched with KI or acrylamide to determine the accessibility of tryptophan residues toward these quenchers. The

TABLE I

ACCESSIBILITY OF THE TRYPTOPHAN RESIDUES IN THE TETRAMERIC AND MONOMERIC PIGEON LIVER MALIC ENZYME

Values shown are averages ± S.E. of two experiments, Trp, tryptophan.

Enzyme association state	Fraction of accessible Trp to KI (α)	Fraction of Trp accessible only to acrylamide (β)	Fraction of Trp inaccessible to both KI and acrylamide (γ)
Tetramer	0.05 ± 0.002	0.15 ± 0.01	0.81 ± 0.02
Monomer	0.25 ± 0	0.16 ± 0.03	0.60 ± 0.03

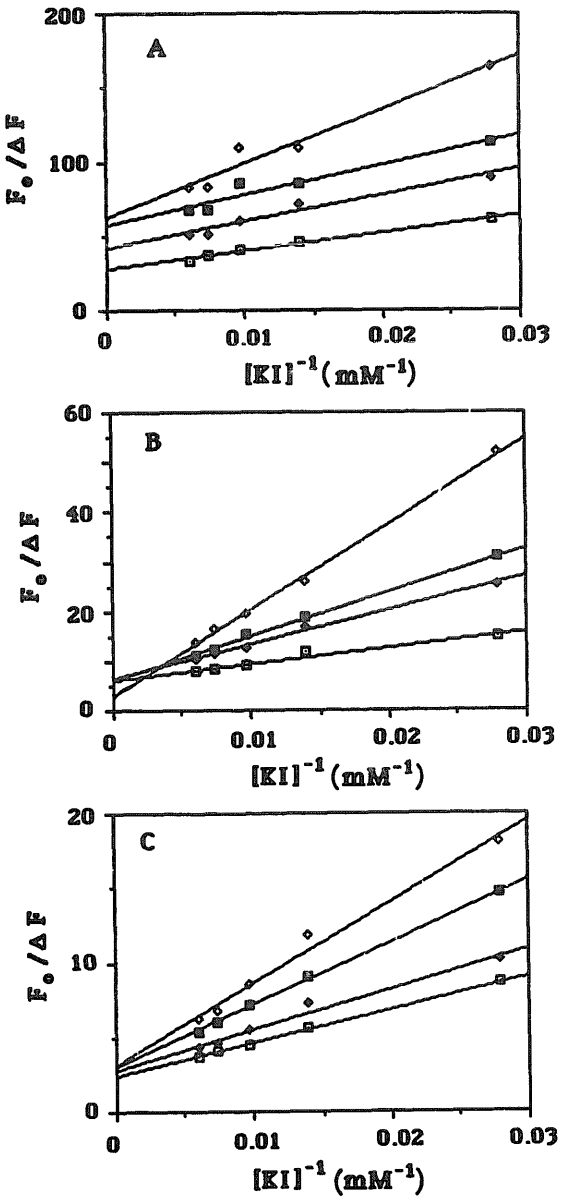

Fig. 6. Double quenching of pigeon liver malic enzyme. The enzyme was simultaneously quenched with KI and acrylamide. The data were treated similarly as in Lehrer's plot, but the slope and intercept represent different fluorescence parameters (see Eqn. 5). (A) Native state; (B) intermediate state (enzyme denatured with 2 M guanidine-HCl); and (C) unfolded state (enzyme denatured with 6 M guanidine-HCl). The acrylamide concentrations were: ◇, 85.5 mM; ■, 57 mM; ◆, 28.5 mM; and □, no acrylamide.

quenching data were fitted to Eqn. 4 for calculating the fractional maximum accessible tryptophan residues and the dynamic quenching constants. Fig. 5A showed the variation of the dynamic quenching constant (K_{sv}) with guanidine-HCl concentration. The biphasic phenomenon was demonstrated again for both KI and acrylamide quenching.

When the quenching experiments were performed with the enzyme at different pH, the K_{sv} vs. pH curve was monophasic (Fig. 5C). Malic enzyme was shown to undergo dissociation at this pH range [4]. The biphasic phenomenon was thus attributed to denaturation and dissociation.

Accessibility of tryptophan residues toward KI (α), acrylamide (β) was also calculated from the Lehrer's plot (Eqn. 4). Biphasic phenomenon was obtained again for α, β or γ (fraction of tryptophan residues inaccessible to both KI and acrylamide) (Fig. 5B). The variation of α or γ with pH was also monophasic (Fig. 5D). β was not varied at different pH. These quenching parameters were less sensitive in visible transitions as shown in Fig. 5; however, they were reliable in characterizing native and denatured states. The quenching parameters for the the tetramer and monomer were summarized in Table I.

Double quenching of malic enzyme fluorescence with KI and acrylamide

Exposed and buried tryptophan residues were also accessed by double quenching technique as described recently by Somogyi et al. [13]. Quenching of malic enzyme denatured to various stages was performed with KI and acrylamide simultaneously. The data were fitted to Eqn. 5. A series of linear plots were obtained. Representative results were presented in Fig. 6 for the native state (6A), intermediate state (6B), and the unfolded state (6C) of the enzyme. The fluorescence quenching parameters for these states of the enzyme were summarized in Table II.

Discussion

Pigeon liver malic enzyme contains 20 tryptophan residues per molecule of enzyme, or five tryptophan residues per subunit [1]. The emission maximum of the enzyme at 328 nm suggested a hydrophobic environment for these residues. However, the shoulder at 340 nm indicated that the tryptophan residues of this enzyme were distributed in two populations: T_{328}, in a hydrophobic environment, and T_{340}, in a more exposed hydrophilic environment. The downward section

TABLE II

FLUORESCENCE PARAMETERS FOR THE NATIVE-, INTERMEDIATE- AND UNFOLDED-PIGEON LIVER MALIC ENZYME

Values shown are averages ± S.E. of two or three determinations.

Enzyme conformation	α	β	γ	K_2 (M^{-1})	K_{1e} (M^{-1})	K_{1i} (M^{-1})
Native	0.05 ± 0.01	0.19 ± 0.02	0.77 ± 0.02	16.8 ± 3.2	8.6 ± 0.3	13.6 ± 5.3
Intermediate	0.19 ± 0.03	0.25 ± 0.04	0.56 ± 0.07	16 ± 1.3	14 ± 1	14.9 ± 5.4
Random coil	0.38 ± 0.01	0.35 ± 0.02	0.26 ± 0.03	12 ± 1	8.1 ± 0.53	16 ± 2

of the Stern-Volmer plot of the quenching data further indicated the heterogeneity of the tryptophan residues in the enzyme molecule [12]. The emission maximum of free tryptophan was near 350 nm. The exceptionally high value of 368 nm observed for malic enzyme reserved further investigation.

Chemical modification of the SH-protected enzyme with *N*-bromosuccinimide, dimethyl(2-hydroxy-5-nitrobenzyl)sulfonium bromide or dimethyl(2-methoxy-5-nitrobenzyl)sulfonium bromide [17] did not cause enzyme inactivation (Chang, unpublished observations). These results suggested a structural rather than a functional role of the tryptophan residues of pigeon liver malic enzyme. These tryptophan residues were buried deeply in the interior of the enzyme molecule and inaccessible to $NADP^+$ [18]. In the present study, we found that the exposed tryptophan residues were for less than 5% in the native state. Over 80% of the tryptophan residues were inaccessible to both KI and acrylamide. The intrinsic protein fluorescence indicated microenvironmental changes of the tryptophan residues. Thus, monitoring the exposure of tryptophan may provide a good indicator for the conformational changes of the enzyme.

Pigeon liver malic enzyme was very sensitive to denaturing conditions. Unfolding of the enzyme in guanidine-HCl followed two phases, as judged by fluorescence quenching, circular dichroism (see Fig. 2) as well as accessible tryptophan residues (Fig. 5). Such a three-state denaturation was observed in many cases [19–22]. For a monomeric protein, biphasic process might suggest that an equilibrium intermediate was involved in the denaturation process. This process was explained by a 'modular assembly or domain folding' model (cf. Ref. 23). In our case, although different probes of secondary (CD) and tertiary structure (fluorescence quenching) each gave similar biphasic transition curves, the modular assembly model might not be applicable; because the enzyme dissociation started at 1.5 M guanidine-HCl, whereas the inflection point was at 2.0 M guanidine-HCl. As judged by the CD variation, the structural order in the protein backbone was not perturbed at guanidine-HCl $\geq$ 1.7 M (Fig. 2), suggesting the integrity of the tertiary structure of the subunits prior to onset of phase II. pH caused reversible dissociation of the enzyme [4]. In this case phase II did not occur. The monomeric forms induced by pH and the intermediate state in the guanidine-HCl titration showed similar accessibility toward KI or acrylamide (Tables I and II). Although protein fluorescence did show some perturbation of the tryptophan environment in phase I as shown in Fig. 2, dissociation of the enzyme subunits by acidic pH induced similar changes (Fig. 5). We concluded that the guanidine-HCl induced biphasic process of pigeon liver malic enzyme was due to enzyme dissociation and denaturation, respectively. The intermediate state represented monomers with minimum conformational changes. The two-phase process corresponded to the following steps: (a) dissociation of the enzyme into subunits with little or no change in tertiary structure and (b) melting-out of the tertiary structure of the subunits.

We have demonstrated that dissociation of the enzyme with pH perturbation was completely reversible [4]. This observation was confirmed by the present study showing that dissociation induced by low concentrations of guanidine-HCl

was also reversible. However, [guanidine-HCl] > 1.5 M caused essentially irreversible denaturation. The above results might suggest that folding of the nascent malic enzyme in vivo was a syntranslational event. The enzyme could not refold to its native conformation even with minimum conformational changes in vitro.

Acknowledgements

We thank Professor Foo Pan for reading this manuscript. This work was supported by the National Science Council, Republic of China (NSC 74-0412-B016-11). Part of this paper is derived from a M.S. thesis presented by H.J.L.

References

1 Nevaldine, B.H., Bassel, A.R. and Hsu, R.Y. (1974) Biochim. Biophys. Acta 336, 283–293.
2 Kam, P.L., Lin, C.C. and Chang, G.G. (1987) Int. J. Peptide Protein Res. 30, 217–221.
3 Hsu, R.Y. (1982) Mol. Cell. Biochem. 43, 3–26.
4 Chang, G.G., Huang, T.M. and Kam, P.L. (1986) in Contemporary themes of biochemistry, ICSU short reports, Vol. VI, pp. 86–87, Cambridge University Press, London.
5 Chang, G.G. and Lee, H.J. (1984) J. Biochem. Biophys. Methods 9, 351–355.
6 Chang, J.T. and Chang, G.G. (1982) Anal. Biochem. 121, 366–369.
7 Hsu, R.Y. and Lardy, H.A. (1967) J. Biol. Chem. 242, 520–526.
8 Hermann, R., Rudolph, R. and Jaenicke, R. (1979) Nature 277, 243–245.
9 Weber, K. and Osborn, M. (1969) J. Biol. Chem. 244, 4406–4412.
10 Lehrer, S.S. and Leavis, P.C. (1978) Methods Enzymol. 49, 222–236.
11 Birdsall, B., King, R.W., Wheeler, M.R., Lewis, C.A., Jr., Goode, S.R., Dunlap, R.B. and Roberts, G.C.K. (1983) Anal. Biochem. 132, 353–361.
12 Lehrer, S.S. (1971) Biochemistry 10, 3254–3263.
13 Somogyi, B., Papp, S., Rosenberg, A., Seres, I., Matko, J., Welch, G.R. and Nagy, P. (1985) Biochemistry 24, 6674–6679.
14 Chang, R.S. and Chang, G.G. (1987) Comput. Methods Prog. Biomed. 24, 37–39.
15 Greenfield, N. and Fasman, G.D. (1969) Biochemistry 8, 4108–4116.
16 Magnuson, M.A., Morioka, H., Tecce, M.F. and Nikodem, V.M. (1986) J. Biol. Chem. 261, 1183–1186.
17 Kita, Y., Fukazawa, M., Nitta, Y. and Watanabe, T. (1982) J. Biochem. (Tokyo) 92, 653–659.
18 Lee, H.J. and Chang, G.G. (1987) Biochem. J. 245, 407–414.
19 Kuwajima, K., Nitta, K., Yoneyama, M. and Sugai, S. (1976) J. Mol. Biol. 106, 359–373.
20 Baig, M.A. and Salahuddin, A. (1978) Biochem. J. 171, 89–97.
21 Robson, B. and Pain, R.H. (1976) Biochem. J. 155, 331–344.
22 Xie, G.F. and Tsou, C.L. (1987) Biochim. Biophys. Acta 911, 19–24.
23 Kim, P.S. and Baldwin, R.L. (1982) Annu. Rev. Biochem. 51, 459–489.